A Role for Fibroblasts in Mediating the Effects of Tobacco-Induced Epithelial Cell Growth and Invasion

Jean-Philippe Coppe[1], **Megan Boysen**[2], **Chung Ho Sun**[2], **Brian J.F. Wong**[2], **Mo K. Kang**[3], **No-Hee Park**[3], **Pierre-Yves Desprez**[1], **Judith Campisi**[1], and **Ana Krtolica**[1]

[1]Life Sciences Division, Lawrence Berkeley National Laboratory, Berkeley, California

[2]University of California Irvine, Irvine, California

[3]School of Dentistry, Center for the Health Sciences, University of California Los Angeles, Los Angeles, California

Abstract

Cigarette smoke and smokeless tobacco extracts contain multiple carcinogenic compounds, but little is known about the mechanisms by which tumors develop and progress upon chronic exposure to carcinogens such as those present in tobacco products. Here, we examine the effects of smokeless tobacco extracts on human oral fibroblasts. We show that smokeless tobacco extracts elevated the levels of intracellular reactive oxygen, oxidative DNA damage, and DNA double-strand breaks in a dose-dependent manner. Extended exposure to extracts induced fibroblasts to undergo a senescence-like growth arrest, with striking accompanying changes in the secretory phenotype. Using cocultures of smokeless tobacco extracts–exposed fibroblasts and immortalized but nontumorigenic keratinocytes, we further show that factors secreted by extracts-modified fibroblasts increase the proliferation and invasiveness of partially transformed epithelial cells, but not their normal counterparts. In addition, smokeless tobacco extracts–exposed fibroblasts caused partially transformed keratinocytes to lose the expression of E-cadherin and ZO-1, as well as involucrin, changes that are indicative of compromised epithelial function and commonly associated with malignant progression. Together, our results suggest that fibroblasts may contribute to tumorigenesis indirectly by increasing epithelial cell aggressiveness. Thus, tobacco may not only initiate mutagenic changes in epithelial cells but also promote the growth and invasion of mutant cells by creating a procarcinogenic stromal environment.

Introduction

Approximately one-third of cancer deaths in the United States are directly linked to tobacco use, and an unknown additional number of cancers are linked to environmental carcinogens in general. In the case of tobacco use, cigarette smoke has been identified as the major cause of cancers of the lung, oral cavity, larynx, and esophagus. Moreover, smokeless tobacco use has been linked primarily to oral cavity cancers, particularly cancers of the cheek and gum (1,2).

Cell culture, animal, and human studies indicate that reactive oxygen species (ROS) and oxidative DNA damage are critical for the pathologies induced by tobacco and other

Disclosure of Potential Conflicts of Interest
No potential conflicts of interest were disclosed.

environmental carcinogens (3–6). Smokeless tobacco extracts increase intracellular ROS levels, and cause DNA fragmentation and lipid peroxidation when administered to rats or human oral keratinocytes in culture (6,7). Higher levels of oxidative DNA damage, assessed by 8-oxo-deoxyguanosine, are also observed in the oral epithelial cells of smokers compared with nonsmokers. Nicotine alone is less efficient at inducing oxidative stress than smokeless tobacco extracts, which contain the same amount of nicotine, indicating that the oxidation reactions caused by the extracts are not due entirely to nicotine (8). In addition to oxidative capacity, smokeless tobacco extracts also have mutagenic activity. This is predominantly due to tobacco-specific nitrosamines (9), strong carcinogens with the ability to form DNA adducts (10). Cell-permeable reactive oxygen scavengers, such as *N*-acetyl-ʟ-cysteine, alleviate the effects of extracts including tissue damage, decrease in collagen contractability, and matrix metalloproteinase (MMP) overexpression, suggesting that intracellular ROS are the main cause of extracts-induced damage (7,11,12). Indeed, when administered orally, *N*-acetyl-ʟ-cysteine inhibited the formation of oxidative DNA adducts (13).

Most studies examining tobacco-induced carcinogenesis focus primarily on mutagenesis of the epithelial cells, the targets of most environmentally induced cancers. However, increasing evidence suggests that stromal-epithelial interactions are crucial for cancer development (14, 15). Stromal cells secrete factors that modulate normal epithelial functions, including proliferation (e.g., during would healing; ref. 16). Moreover, activated or reactive stroma can fuel the growth and progression of abnormal, premalignant, or malignant epithelial cells (17–19).

A few reports suggest that tobacco constituents may alter the secretory phenotype of stromal fibroblasts. For example, at concentrations present in the saliva of smokeless tobacco users, nicotine inhibits the synthesis of collagen I, collagen II, and fibronectin, and induces collagenase activity in human gingival fibroblasts (20). Likewise, tobacco extracts significantly reduce the ability of human skin fibroblasts to synthesize collagen and fibronectin and contract collagen gels by inducing the synthesis of MMP-1 and MMP-3. These effects were inhibited by reactive oxygen scavengers, indicating the mediation by ROS (11,12). These results suggest that tobacco constituents may contribute to the development of cancer not only through their mutagenic effects, but also through ROS-mediated changes in the secretory phenotype of stromal fibroblasts. Consistent with this idea, smokeless tobacco extracts, at least at low doses, stimulated keratinocytes to proliferate in three-dimensional skin raft cultures (21). This stimulation might have been indirect, via stromal components of the raft cultures, although this was not determined directly. On the other hand, nicotine-treated epithelial cells inhibited the growth and collagen production by fibroblasts in two-chamber coculture experiments, suggesting that tobacco constituents can alter epithelial-stromal interactions through soluble factors secreted by tobacco-exposed cells (22).

Although some aspects of tobacco-induced tumorigenesis are well established, the potential importance of epithelialstromal interactions in this process remains largely unknown. Here, we present evidence that tobacco alters the secretory phenotype of fibroblasts, enabling them to increase the proliferation and invasion of epithelial cells. Our findings add a new and potentially important dimension—nonmutagenic activation of stromal pathways—to our understanding of how noxious environmental agents might promote cancer.

Results

Effects of Smokeless Tobacco Extract on Proliferation of Fibroblasts

We first determined whether and how smokeless tobacco extract (Tob) affects the proliferation of skin and oral fibroblasts. We chose a range of Tob concentrations similar to those which smokeless tobacco users experience in saliva, as measured by nicotine content (9), because it

is likely that in damaged areas of mucosal tissue, the stroma experiences tobacco concentrations at or near those found in saliva. We treated normal human skin (82.6) and oral fibroblasts (NHOF) with Tob concentrations ranging from 0.1% to 8% continuously for intervals ranging from 1 to 10 days, monitoring cell morphology by phase contrast microscopy and cell proliferation by the number of cells and the fraction that incorporated radiolabeled thymidine. Cells exposed to 8% and 6% of Tob began rounding up and exhibiting signs of apoptosis within the first 24 and 72 hours, respectively; however, fibroblasts exposed to 4% and lower concentrations showed no significant signs of cell death for up to 10 days (data not shown). Interestingly, by day 4, cells exposed to 1% to 4% of Tob showed signs of enlargement and increased spreading (Fig. 1A), a morphology reminiscent of a senescence-like state (23).

We monitored the proliferative status of control and Tob-exposed fibroblasts by their cumulative number (Fig. 1B) and ability to incorporate [^{3}H]thymidine into nuclear DNA (Fig. 1C–E), detectable by autoradiography and 4′,6-diamidino- 2-phenylindole (DAPI) staining (labeling index). Control fibroblasts grew continuously for ~4 days before ceasing growth upon reaching confluence. By contrast, fibroblasts treated with 1%, 2%, 4%, 6%, or 8% of Tob ceased growth after ~2 days (Fig. 1B). Fibroblasts exposed to 0.1% of Tob grew nearly as well as control cells. As expected, the number of cells treated with 6% and 8% of Tob began to decline 1 and 3 days after exposure due to cell death. However, the number of cells treated with 1%, 2%, or 4% of Tob remained constant after the first 2 days, and this cessation in proliferation was accompanied by a decline in the labeling index, indicating an arrest of cell growth (Fig. 1B and C).

Within the range of sublethal doses, both the interval and level of Tob exposure influenced the kinetics and reversibility of the growth arrest. For example, ~60% of cells exposed to 4% of Tob for 1 day resumed growth after removing Tob from the medium, an effect close to the 55% achieved by a 2-day exposure to 2% of Tob (Fig. 1D). After 4 days, a 2% and 4% Tob exposure irreversibly arrested the growth of 90% of the population (data not shown). After 6 days, only fibroblasts exposed to 1% of Tob were able to resume growth and even then the recovery was only partial (50%; Fig. 1E). At higher Tob concentrations (e.g., 4%), >99% of the fibroblast population arrested growth irreversibly after a 6-day exposure (Fig. 1E), an effect achieved by a 10-day exposure to 2% of Tob (data not shown). Therefore, smokeless tobacco extracts induced an irreversible growth arrest that depended on both the dose and the time-dependent cumulative effect, a situation likely to occur during multiple exposures *in vivo*.

Smokeless Tobacco Extracts Induce ROS Production and Oxidative DNA Damage in Fibroblasts

Tobacco smoke and smokeless tobacco extracts contain multiple DNA-damaging compounds, including producers of ROS (24). Oxidative damage can arrest the growth of a variety of cell types (25). In human fibroblasts, oxidants are thought to arrest growth irreversibly with features of cellular senescence owing primarily to DNA damage (26). Thus, the growth arrest caused by smokeless tobacco extracts might be due to extracts-produced ROS and subsequent DNA damage. To address this possibility, we measured intracellular ROS production by fibroblasts exposed to 0.1%, 1%, 2%, or 4% of Tob for intervals ranging from 2 hours to 6 days. Tob increased intracellular ROS levels in a dose-dependent manner after 2 hours (Fig. 2A). Interestingly, longer exposures did not further increase the ROS levels; rather, ROS levels were significantly lower after exposure times of 24 hours and 6 days for doses of 1% or greater. This decline was not due to the inactivation of Tob by cell-independent processes because preincubation of the extract for 24 hours at 37°C did not diminish its ability to increase ROS within 2 hours (data not shown). We speculate that the decline in ROS levels may be due to an up-regulation of antioxidant defenses in the cells. After replacement of the Tob-containing medium with control medium, intracellular ROS decreased to control levels within 24 hours.

This result indicates that the irreversible growth arrest caused by high levels or prolonged exposure to smokeless tobacco extracts is not due to the continued production of ROS.

To determine whether the increased ROS levels produced by Tob cause oxidative DNA damage, we used the Fpg-FLARE Comet Assay. In this assay, the length of the comet tail is directly proportional to the amount of oxidative DNA damage in the cell. The average comet tail length was significantly longer in the fibroblasts exposed for 42 hours to 2% or 4% of Tob compared with control fibroblasts (Fig. 2B). Moreover, the fraction of nuclei that formed significant tails ($\geq$10 µm) increased 3-fold and 7-fold, respectively, in cells exposed to 2% and 4% of Tob (Fig. 2C). In addition, the frequency of cells with longer tails ($\geq$20 µm) also increased in a dose-dependent manner. Whereas only 2% of control cells had long tails, 6% (3-fold increase) and 26% (13-fold increase) of fibroblasts exposed to 2% and 4% of Tob, respectively, had long tails. These results indicate that smokeless tobacco extracts induce oxidative stress in exposed fibroblasts, and this stress leads to an accumulation of oxidative DNA damage.

To establish whether this oxidative damage results in DNA double-strand breaks (DSB), only a single one of which is required to induce an irreversible senescence arrest (27), we immunostained control fibroblasts and cells exposed to 1%, 2%, or 4% of Tob for 6 days for nuclear foci containing phosphorylated histone H2AX (γH2AX) and 53BP1. The H2AX histone H2A variant is phosphorylated in chromatin flanking broken DNA and is commonly used as an early marker of DNA DSBs (28). 53BP1 is an adaptor protein for DNA repair complexes, and colocalizes with γH2AX at the damaged DNA (29). The number of γH2AX foci per nucleus increased sharply in Tob-exposed fibroblasts, suggesting that Tob induces DNA DSBs (Fig. 3A). Consistent with this interpretation, >90% of the γH2AX foci formed by Tob colocalized with 53PB1 (Fig. 3B). The number of γH2AX foci per nucleus increased with increasing Tob concentration (Fig. 3C).

To examine whether Tob-induced DNA damage was reversible, we incubated fibroblasts with 4% of Tob, then allowed them to recover in the absence of Tob for 6 days. Immunostaining for γH2AX and 53BP1 foci (Fig. 3B and D) showed that Tob-treated cells accumulated γH2AX foci whether exposed for 2 hours, 24 hours, or 6 days. After the 6-day recovery period, cells exposed for 24 hours had only slightly more foci than untreated control cells. By contrast, cells exposed for 6 days retained substantial levels of γH2AX foci after the 6-day recovery period. This Tob concentration and exposure time correlated well with the levels and exposure times necessary to induce permanent growth arrest. We also noticed that the average size of γH2AX foci increased in these cells, resembling the large γH2AX foci that have been observed in replicatively senescent fibroblasts (30).

Smokeless tobacco extracts also induced markers of DNA damage in reconstructed skin rafts. These three-dimensional cocultures containing keratinocytes and fibroblasts form structures that resemble human skin, containing a stratified epithelium supported by an underlying fibroblast-containing stroma. We exposed differentiated raft cultures to 4% of Tob extract and immunostained for γH2AX foci. Tob induced γH2AX foci, indicative of DNA DSBs, in both fibroblasts and keratinocytes within the rafts (Fig. 3E and F). We also noticed a significant decrease in keratinocyte stratification upon exposure to tobacco and this effect also correlated with the tobacco concentration (data not shown).

Taken together, these results show that once a threshold level of Tob exposure is reached, fibroblasts undergo an irreversible growth arrest reminiscent of senescence, which can be induced by DNA damage (oxidative lesions and DSBs; refs. 31–34). At higher Tob exposure levels, cells die, as previously reported (35).

Smokeless Tobacco Extracts Alter the Secretory Phenotype of Fibroblasts

Fibroblasts that have undergone a senescence arrest in response to DNA damage or replicative exhaustion alter their secretory phenotype (senescence-associated secretory phenotype or SASP; refs. 36–38).[4] We asked whether this was also the case for Tob-treated fibroblasts that displayed a senescent-like growth arrest. We therefore collected conditioned medium from control fibroblasts and fibroblasts exposed to 1%, 2%, or 4% of Tob for 6 days. We normalized the samples for cell number and analyzed them for specific secreted proteins using substrate gel zymography, antibody arrays, and Western blotting.

A major change in the fibroblast secretory phenotype upon senescence is increased secretion of MMPs. We therefore analyzed the conditioned media for MMP activities. Gelatin is efficiently degraded by the type IV collagenases (such as MMP-2), whereas casein is a better substrate for the stromelysin family MMPs (such as MMP-3). Compared with control cells, Tob-exposed fibroblasts secreted higher levels of active MMP-2 (72 kDa gelatinase) and MMP-3 (stromelysin-1; refs. 39,40). Results obtained by zymography were confirmed by Western blotting (Fig. 4A). Tobacco exposure was reported to induce MMP-1 (collagenase 1) expression (11). In our hands, MMP-1 secretion was not affected by Tob, although replicatively senescent fibroblasts exhibited higher MMP-1 secretion (data not shown) as reported (37). This discrepancy might be due to differences in how MMP-1 levels were measured—we examined secretion, whereas the Yin et al. study measured mRNA levels.

To more broadly assess the Tob-induced secretory phenotype, we analyzed conditioned medium using antibody arrays. Although limited by the antibodies present on the array, the commercially available array we used had the ability to detect 120 secreted proteins, including a variety of cytokines and growth factors. Table 1 lists the secreted proteins for which we observed the most prominent reproducible changes upon exposure to Tob. We confirmed the expression of three of the most highly up-regulated proteins, the insulin-like growth factor-binding factor 4 (IGFBP4) as well as the tissue inhibitors of MMPs (TIMP-1 and TIMP-2), by Western blotting (Fig. 4B). We also listed macrophage inflammatory protein-1a (MIP-1a), an example of a protein that showed little or no change in abundance in the conditioned medium from control and Tob-exposed cells. Relative to the control cells, smokeless tobacco extracts induced a moderate secretion of proteins such as basic fibroblast growth factor, as well as cytokines involved in inflammatory response. We speculate that increased secretion of inflammatory cytokines may contribute to the chronic inflammation often observed in the oral mucosa and respiratory tract of tobacco users.

Soluble Factors Secreted by Tobacco-Exposed Fibroblasts Stimulate Proliferation of Skin and Oral Keratinocytes

We previously showed that senescent fibroblasts stimulate the growth of preneoplastic epithelial cells in culture and mice (41), and disrupt the function of normal epithelial cells in three-dimensional cultures (42). To determine whether Tob-induced changes in fibroblasts could alter epithelial cell proliferation, we used three coculture systems, as previously described (41): (*a*) direct cocultures (epithelial cells seeded directly over fibroblasts), (*b*) indirect cocultures (epithelial cells plated in the upper chambers of two-chamber transwells, with fibroblasts plated in the lower chambers), and (*c*) culture on deposited extracellular matrix (epithelial cells seeded onto the extracellular matrix deposited by fibroblasts). We used two types of immortalized keratinocytes: HaCAT isolated from human skin, and DOK isolated from dysplastic lesions in oral epithelium. Fibroblasts were treated with 1%, 2%, or 4% of Tob for 6 days and prepared for cocultures (as described in Materials and Methods).

---

[4]Coppe et al., submitted for publication.

Relative to control cells, oral fibroblasts (NHOF) exposed to Tob for 6 days stimulated HaCAT proliferation 2-fold to 3-fold in direct cocultures, with the degree of stimulation increasing with increasing Tob dose to which the fibroblasts were exposed (Fig. 5A and B). Similar results were obtained when HaCAT cells were cocultured with Tob-treated skin (82.6; Fig. 5B, *left*) and foreskin (BJ; data not shown) fibroblasts. Moreover, Tob-exposed NHOF (82.6; Fig. 5C) and BJ fibroblasts (data not shown) stimulated the proliferation of DOK epithelial cells. For 1% and 2% Tob exposure, the effects observed in direct cocultures were also seen in indirect cocultures, which allow only soluble fibroblast-derived factors to reach the epithelial cells. However, whereas 4% of Tob-exposed fibroblasts induced even higher HaCAT growth in direct cocultures, this was not the case in indirect cocultures (Fig. 5B versus D). One possible explanation for this difference is that 4% of tobacco induces changes in the fibroblast extracellular matrix composition, which in turn, modifies the availability of soluble growth factors. Interestingly, we observed no differences in the growth of HaCAT and DOK cells cultured on extracellular matrix from Tob-exposed and control fibroblasts (Fig. 5E). This suggests that the growth stimulation was probably due to soluble factors secreted by Tob-altered fibroblasts.

Next, we cocultured normal human primary oral or skin keratinocytes with the control or Tob-exposed fibroblasts and examined proliferation. Interestingly, we did not observe any stimulation of keratinocyte proliferation in the presence of tobacco-exposed fibroblasts (data not shown). This suggests that preneoplastic changes in keratinocytes are necessary in order to sensitize them to stimulation by Tob-arrested fibroblasts. Taken together, these data support the idea that Tob-altered fibroblasts may stimulate the aggressive phenotype of immortalized epithelial cells by secreting soluble growth-promoting factors.

Smokeless Tobacco Extracts –Exposed Fibroblasts Stimulate Interstitial Invasion of Oral Epithelial Cells

Because tobacco exposure induced the secretion of matrix-degrading enzymes, we hypothesized that the Tob-altered secretory profile might affect epithelial cell invasiveness. Therefore, we performed basement membrane and interstitial invasion assays in the presence of the conditioned medium from control or Tob-exposed fibroblasts.

Relative to control conditioned medium, conditioned medium from 2% and 4% Tob-exposed fibroblasts stimulated DOK invasiveness 2.4-fold and 4-fold, respectively (Fig. 5F). However, HaCAT invasion was unaffected, even when the assay was extended from 16 to 24 hours (data not shown). These data suggested that in addition to the increased availability of MMPs and possibly other factors, HaCAT cells would need additional factors in order to acquire an invasive phenotype. In contrast, DOK cells seemed to be susceptible to Tob-induced secreted factors with respect to acquiring invasiveness. HaCAT have strong cell-cell interactions and form a more polarized epithelium than DOK, supporting the idea that DOK are more dedifferentiated. Fibroblast stimulation of invasiveness was directly proportional to the extent of the smokeless tobacco extracts exposure. This is in accordance with the dose-dependent changes in secretory phenotype (Fig. 4).

Consistent with their noninvasive phenotype, HaCAT did not invade basement membrane, even when Matrigel was diluted to 5% (Fig. 5G), whether or not conditioned medium from Tob-exposed fibroblasts was present. On the other hand, DOK cells invaded the basement membrane, albeit only when Matrigel was diluted to 25%, but conditioned medium from Tob-exposed fibroblasts did not stimulate this weakly invasive phenotype. Similar results were obtained using another weakly invasive keratinocyte cell line, HSC-3, although there was a reproducible, albeit not significant, trend towards higher invasiveness in the presence of 4% of Tob conditioned medium (Fig. 5G). Thus, whereas Tob-exposed fibroblasts secreted factors

that stimulated some epithelial cells to invade the interstitial collagen, they could only weakly stimulate their ability to invade a basement membrane.

Smokeless Tobacco Extracts –Exposed Fibroblasts Down-Regulate Cell Polarization and Keratinization Markers

In addition to increased proliferation, keratinocytes grown on Tob-exposed fibroblasts displayed an altered morphology, appearing flatter and showing less prominent cell-cell contacts (Fig. 5A). We therefore examined HaCAT cells grown on control, 1%, 2%, or 4% of Tob-treated fibroblasts for tight junctions and adherens junctions (Fig. 6).

Epithelial colonies on Tob-treated fibroblasts showed a dramatic decrease in the tight junction marker ZO-1, as determined by immunofluorescence (Fig. 6A and B). This decrease was Tob dose–dependent (data not shown). In addition, E-cadherin immunostaining at the cell membrane also decreased, indicating a lack of adherens junctions (Fig. 6C and D). Nuclear DAPI staining indicated that colonies on Tob-exposed fibroblasts were less compact than colonies on control fibroblasts (Fig. 6E and F). To quantify these changes, we prepared extracts from cocultures containing enhanced green fluorescent protein– expressing HaCAT cells grown on control fibroblasts or fibroblasts exposed to 1%, 2%, or 4% of Tob for 6 days, and Western blotting was done (Fig. 6G, Table 2). Tob-exposed fibroblasts reduced E-cadherin, β-catenin, and involucrin abundance in the epithelial cells in a dose-dependent manner. Although all three proteins were down-regulated, the extent and the pattern of down-regulation varied significantly with Tob exposure of the fibroblasts. For example, although E-cadherin abundance decreased 2.5-fold in the presence of 1% Tob-exposed fibroblasts, it was only slightly more reduced by 2% Tob exposure but declined 6-fold in the presence of 4% Tob-exposed fibroblasts. In comparison, β-catenin was reduced by 1% and 2% Tob-exposed fibroblasts similarly to E-cadherin, but unlike E-cadherin, did not decline further when HaCAT cells were cultured on 4% Tob-exposed fibroblasts. These data indicated that different proteins expressed by the epithelial cells were likely independently affected by tobacco-exposed fibroblasts. Interestingly, normal keratinocytes showed no decrease in E-cadherin or change in cell morphology upon coculture with Tob-exposed fibroblasts (data not shown), suggesting that the effects of tobacco-modified stroma were limited to immortalized epithelial cells.

Discussion

In this article, we examine the direct effects of smokeless tobacco extracts on human oral fibroblasts as well as the indirect effects on human epithelial cell phenotype. Although it is evident that both stromal and epithelial cells are simultaneously exposed to tobacco *in vivo*, we present here *in vitro* data that suggest significant effect of fibroblast enzyme on epithelial cell behavior. We hypothesize that irreversible alterations in stromal cells (which have a much slower renewal rate than oral epithelial cells) may exert a continuous effect on the faster renewing epithelial cells, and therefore may stimulate tumor promotion and progression even in the absence of further exposure.

Exposure of skin and oral fibroblasts to smokeless tobacco extracts induces ROS in a dose-dependent manner and leads to oxidative DNA damage and DSBs. Once the level of damage is above the ability of the cells to repair, it induces permanent growth arrest and changes in the secretory phenotype reminiscent of the senescence response. Interestingly, smokeless tobacco extracts and other known senescence inducers, such as hydrogen peroxide and telomere dysfunction, share the ability to activate DNA damage response in cells and cause an accumulation of DNA damage foci. However, some features of the extracts-arrested fibroblasts, such as weak senescence– associated β-galactosidase staining (data not shown), seem unique to the arrest caused by smokeless tobacco extracts. We speculate that this will be a common theme once detailed analyses of different senescence-like states is performed. There

may be core features shared by all senescence inducers, whereas other characteristics may be specific for subgroups of inducers.

We have shown that factors secreted by senescent fibroblasts can stimulate epithelial cell proliferation and disrupt epithelial differentiation (41,42). The proliferative effects of senescent fibroblasts were independent of senescence inducers, and depending on the assay, were in some cases limited to initiated, immortalized epithelial cells. Here, we show that, like senescent fibroblasts, tobacco-exposed fibroblasts stimulated the proliferation of immortal keratinocytes in two-dimensional direct coculture assays. However, senescent fibroblasts had no effect on normal epithelial cells (data not shown). This is similar to the effects we observed in two-dimensional cocultures with replicatively senescent fibroblasts (41).

Our results show that tobacco may alter epithelial tissue integrity by reducing expression and membrane localization of critical cell junction proteins E-cadherin and ZO-1. This is consistent with two reports showing that tobacco exposure increases the permeability of the respiratory epithelium and leads to the deterioration of E-cadherin and tight junctions in animal models (43,44). Interestingly, methylation of the E-cadherin promoter is a common event (36%) in squamous cell carcinoma of the head and neck, suggesting its importance in carcinogenesis (45). Indeed, E-cadherin down-regulation has been associated with dedifferentiation, invasion, and metastasis of squamous and other carcinomas (46–48). Our results suggest that tobacco exposure may reduce E-cadherin in the epithelium by yet another epigenetic mechanism— stimulating the secretion of stromal factors that promote loss of E-cadherin expression and localization.

Although the link between tobacco use and cancer development is well established, the mechanisms involved in tobacco-related carcinogenesis remain only partially understood. Recent studies have shown a reduced growth rate for lung fibroblasts in patients with pulmonary diseases and an up-regulation of two pathways linked to cell senescence, p53 and p16 (49,50). These data suggested that multiple exposures to cigarette smoke could move lung fibroblasts into an irreversible state of senescence. However, most research in this area has concentrated on the mutagenic properties of tobacco constituents and their ability to induce mutations necessary for the malignant transformation of epithelial cells, which give rise to the majority of cancers (4,51). Although there is little doubt that mutations are essential for tumorigenesis, an increasing body of evidence suggests that changes in the microenvironment of tumor cells contribute significantly to tumor progression and possibly to initiation (14,15, 38).

In this study, we show that tobacco-exposed fibroblasts disrupt epithelial cell-cell interactions and stimulate epithelial migration and proliferation. According to our results, a likely scenario for tobacco-related cancer development would be that, with tobacco use, the epithelium acquires mutations due to direct exposure to mutagenic substances present in tobacco (52). These mutations are fixed efficiently because of the relatively high proliferation of the epithelial cells. At the same time, exposure of the stroma to tobacco may cause an accumulation of permanently arrested stromal fibroblasts, which exhibit an altered secretory phenotype. Cells within epithelial stem or progenitor cell pools that harbor mutations conferring a growth and/ or survival advantage are stimulated to proliferate and invade by the presence of tobacco-arrested fibroblasts. The procarcinogenic environment may continue to promote the tumor progression of these initiated cells, even in the absence of continued tobacco exposure. Overall, our findings suggest a novel mechanism by which a damaged stroma in general, caused by exogenous or endogenous stresses and/or aging, may contribute to tumorigenesis.

Materials and Methods

Cell Culture

Fibroblasts and epithelial cells were cultured as previously described (41).

Fibroblasts

Normal human fibroblasts from skin (82.6, from J. Oshima, Dept. of Pathology, University of Washington, Seattle, WA; and BJ, from the American Type Culture Collection), oral mucosa (NHOF, from N.H. Park, Dept. of Dentistry, University of California at Los Angeles, Los Angeles, CA) or embryonic lung (WI38, from American Type Culture Collection) were maintained in DMEM (Life Technologies-Invitrogen) supplemented with 10% fetal bovine serum (Tissue Culture Biologicals), penicillin-streptomycin (5 units/L; Sigma), and glutamine (L-Gln 2 mmol/L; Life Technologies-Invitrogen). The fraction of proliferating cells was monitored by [3H]thymidine incorporation as previously described (41). Presenescent cultures contained >85% proliferating cells. Senescent cultures contained <10% proliferating cells.

Epithelial cells

We used two nonmalignant keratinocyte cell lines: DOK, isolated from a dysplastic oral mucosa (53), and HaCAT, a spontaneously immortalized keratinocyte line from skin (54). We also used normal human epidermal keratinocytes (NHEK; Cambrex), and an invasive keratinocyte cell line, HSC-3, from an oral squamous cell carcinoma (55). Cells were cultured as previously described (53–55). Briefly, HaCAT and NHEK were cultured in keratinocyte growth medium (keratinocyte basal medium containing 0.4% bovine pituitary extract, 5 µg/mL insulin, 0.1 µg/mL epidermal growth factor, 0.5 µg/mL hydrocortisone, and 0.075 mmol/L $CaCl_2$; Cambrex), whereas DOK and HSC-3 were cultured in DMEM supplemented with 10% fetal bovine serum, penicillin-streptomycin (5 units/L; Sigma), and glutamine (L-Gln 2 mmol/L; Life Technologies-Invitrogen).

Tobacco Extract (Tob) and Treatment

The smokeless tobacco extract was prepared as previously described (56). Chewing tobacco (Copenhagen Snuff-U.S. Smokeless Tobacco, Co.) was divided into 5-g portions and crushed for 5 min at room temperature in 5 mL of serum-free DMEM. DMEM was added to a final concentration of 10% w/v. The tobacco-DMEM mixture was incubated for 2 h at 37°C with shaking. The supernatant was clarified twice by centrifugation at 5,000 rpm in a sw4 rotor (Sorwall) for 5 min. After adjustment to pH 7.4 with 2 mol/L of HCl, the extract was filtered (0.45 µm; Nalgen Nunc International). This extract, which we term Tob, was stored at 4°C and used within 1 month, an interval over which we did not observe any differences in biological activity with respect to the effects we measured. Prior to fibroblast exposure, Tob was diluted with DMEM to the desired concentration and supplemented with 10% fetal bovine serum, unless noted otherwise. To adjust for effects of Tob on cell growth, fibroblasts were seeded onto 100 mm dishes 1 day prior to exposure at 1×10^5 for controls, and 2×10^5, 3.5×10^5, or 5×10^5 for exposure to 1%, 2%, or 4% of Tob, respectively. Replicatively senescent fibroblasts were seeded at 5×10^5.

Fibroblast Proliferation

Fibroblasts were seeded at 1.5×10^4 per well in six-well dishes 1 day prior to Tob exposure. Cell proliferation was monitored by [3H]thymidine incorporation and nuclear DAPI staining (1 µg/mL DAPI in PBS; Sigma) as previously described (41). [3H]Thymidine (10 Ci/mL; 60–80 Ci/mmol; Amersham) was added for the last 20 h of culture. After fixation in 95% ethanol, radioactive nuclei were exposed to a photographic emulsion, the emulsion was developed and nuclei were counterstained with DAPI. Wells were scored by phase-contrast for dark [3H]-

labeled nuclei and DAPI fluorescence (all nuclei). Cell number was determined by counting the number of DAPI-stained nuclei in five random fields per well (400–800 cells per data point). The labeling index was expressed as the percentage of radioactively labeled (dark) nuclei relative to the total number of DAPI-stained nuclei.

ROS Measurement

H_2DCFDA (DCFH-DA, Molecular Probes; C-400), was solubilized in DMSO (10 mmol/L). Modified Eagles medium (MEM) containing 20 µmol/L of DCFH-DA was equilibrated in a cell culture incubator for 4 h. Control and experimental cells were cultured in 60 mm dishes and incubated with 4 mL of equilibrated DCFH-DA medium for the last 2 h of control or Tob treatment. Cells were washed, detached by trypsinization, and immediately analyzed by FACS. Samples were normalized to a control that contained the same concentration of DMSO but no DCFH-DA. Cells treated with 100 µmol/L of hydrogen peroxide for 1 h served as a positive control. A correlation between DCFH-DA–produced fluorescence and ROS production was confirmed by exposing cells to increasing doses of hydrogen peroxide. The fluorescence intensity measured by FACS was directly proportional to the hydrogen peroxide dose.

Fpg-FLARE Comet Assay

Fpg-FLARE Comet Assay (Fpg-formamidopyrimidine DNA glycosylase; FLARE-fragment length analysis using repair enzymes) was done using a kit (Trevigen), as previously described (57). Comet tail lengths of 50 randomly chosen nuclei per sample were measured using the Comet macro (58) in the Scion Image program, and average tail lengths were calculated. For each experimental point, at least two independent cultures were analyzed. Oxidative DNA damage was estimated by subtracting the mean tail length of the untreated from that of the Fpg-treated sample (normalized mean tail length). Results are depicted as the average tail length and distribution of mean tail lengths for each sample.

Zymography

Conditioned medium from fibroblasts exposed to Tob was collected, concentrated 175-fold to 200-fold using Vivaspin (10 kDa cutoff, Vivascience), and diluted with PBS to normalize for cell number. Normalized conditioned medium (10 µL) was mixed with 5 µL of 3× nonreducing Laemmli sample buffer and incubated at 37°C for 15 min. The mixture (7.5 µL) was analyzed on casein and gelatin substrate polyacrylamide gels (12% PAGE casein; 10% PAGE gelatin; Bio-Rad) as previously described (59). After electrophoresis, gels were activated for 1 h in 2.5% Triton X-100 at room temperature, followed by overnight incubation in substrate buffer [100 mmol/L Tris-HCl (pH 7.4), 15 mmol/L $CaCl_2$]. The gels were stained with Coomassie blue for 30 min and destained with 30% methanol/10% acetic acid. Caseinase and gelatinase activities were visible as clear bands.

Western Blotting

Protein cell extracts were prepared in reducing Laemmli sample buffer and Western blotting was done as previously described (57,59). Briefly, 15 to 35 µg of cell protein or 15 µL of normalized concentrated conditioned medium were separated by SDS-PAGE using 7.5% or 12% acrylamide gels and blotted onto nylon membranes. The membranes were blocked and probed either overnight at 4°C or 1 h at room temperature with primary antibody. After washing, membranes were incubated with horseradish peroxidase–labeled secondary antibodies (1:3,000 dilution), and protein bands were detected using ECL or ECLPlus (Amersham Biosciences). Band intensities were quantified using ImageQuant Software (Molecular Dynamics). To simplify normalization for epithelial cell number, some cocultures were prepared using enhanced green fluorescent protein–labeled epithelial cells and Western blots were normalized for epithelial cell number using antibodies to enhanced green fluorescent

protein. Alternatively, the epithelial marker cytokeratin-14 served to normalize for epithelial cell number. Both normalization methods yielded similar results.

Immunofluorescence

Cells were cultured in six-well dishes on glass coverslips and exposed to Tob. Cells were fixed with formaldehyde 4% (Sigma) for 20 min, washed with PBS, permeabilized for 5 min with 0.5% Triton X-100, washed, and either used immediately or dehydrated for 5 min with 100% methanol and kept at −20°C. Coverslips were blocked for 1 h with 10% goat serum, incubated with primary antibody for 1 h at room temperature or overnight at 4°C, washed and incubated with a 1:500 dilution of goat secondary antibody (Alexa Fluor, Molecular Probes) for 45 min at room temperature. After washing, samples were mounted and examined by epifluorescence microscopy.

Antibodies

The primary antibodies and dilutions used for Western blotting were MMP-1 (Ab-1) and MMP-2 (Ab-3) at 1:100, MMP-3 (Ab-5) at 1:200 (mouse; Oncogene), IGFBP4 at 1:250 (goat; Santa Cruz Biotechnology), E-cadherin at 1:100 (mouse; Translab), β-catenin at 1:750 (mouse; Translab), involucrin at 1:100 (mouse; NeoMaker), cytokeratin-14 at 1:150 dilution (mouse; NovoCastra), and TIMP-1 (rabbit, Santa Cruz Biotechnology) and TIMP-2 (mouse, R&D Systems) at 1:500 dilution. Primary antibodies and dilutions used for immunocytochemistry were zona occludens protein-1 (ZO-1) at 1:200 (mouse; Dako), E-cadherin at 1:100 (mouse; Translab), 53BP1 at 1:1,000 (rabbit; Bethel Laboratories), and γH2AX (mouse; Upstate Biotechnology) at 1:1,000 dilution.

Antibody Array Analyses

Control or Tob-treated cells were incubated for 2 days in serum-free medium. Conditioned medium was collected, cells were counted, and samples were concentrated 2-fold to 3-fold using centrifugation filters with a 3 kDa cutoff (Millipore, Co., Amicon; Centriplus YM-3) at 4°C. DMEM was used to normalize the conditioned medium volume to the equivalent of 1.5×10^5 cells. Normalized conditioned media were used to probe membranes containing immobilized antibodies (RayBiotech; RayBio Human Cytokine Antibody Array C Series 1000), according to the manufacturer's instructions. Briefly, membranes were blocked for 30 min, incubated with conditioned medium for 1 h at room temperature, and washed five times. Membranes were then incubated with a mixture of biotin-conjugated antibodies (overnight, 4°C), washed five times, incubated with horseradish peroxidase–conjugated streptavidin (1.5 h, room temperature), washed five times, and detected by chemiluminescence (ECLPlus). Multiple exposures of the film were obtained for each membrane. Comparative analysis of the proteins detected on the arrays was made by scanning developed films, transforming the control samples into red (and Tob-treated samples into green) using image editing software (Adobe Photoshop). We overlapped the colored images, and scored signals for predominantly green (increased in Tob-exposed samples), predominantly red (decreased in Tob-exposed samples), or yellow (no significant difference between samples). Only signals showing the same color and intensity ±10% in duplicate spots on the same array were considered. For each condition, three independently collected samples of conditioned medium were analyzed on separate arrays. Based on the intensity and color of the spots, the relative abundance of proteins was ascribed as: −, no detectable signal above background; +/−, signal above the background level, but less than double intensity of the background; +, ++, +++, signals above background, where ++ signifies 150% to 250% higher signal than + and +++ depicts 250% to 500% higher signal than +. Results depict changes duplicated (same number of + signs assigned) in at least two of the three samples.

Cocultures

Fibroblasts were pretreated with Tob for 5 days in complete culture medium, and replated onto six-well dishes at 8×10^4 cells per well for controls and 1.2×10^5 cells per well for Tob in order to achieve similar degrees of confluence. Cells were allowed to attach for 4 h, then were treated with Tob for an additional day for direct and indirect cocultures, or 3 additional days to generate the extracellular matrix. After washing, 2×10^4 epithelial cells were seeded directly onto the fibroblasts for direct cultures, or into the upper chamber of two-chamber transwells for indirect cocultures (Millicells-PCF, Millipore). For matrices, fibroblasts were removed with 0.5 mmol/L of EDTA (Versene, Life Technologies-Invitrogen) prior to washing and seeding 2×10^4 epithelial cells. All cocultures were done in keratinocyte growth medium (Cambrex) supplemented with $CaCl_2$ to a final concentration of 1.375 µmol/L.

Epithelial Cell Proliferation in Cocultures

Epithelial cells were infected with the retrovirus pLXSN-EGFP (expressing enhanced green fluorescent protein) and selected for 7 days in G418 (Sigma) as previously described (41). Enhanced green fluorescent protein was expressed in >90% of the cells. To quantify the growth of epithelial cells in cocultures, green fluorescent images from five to eight random fields per well (250–500 epithelial cells per data point) were captured at 40× magnification (41,60).

Boyden Chamber Invasion Assays

Assays were done in modified Boyden chambers with 8-µm pore filter inserts for 24-well plates (BD Bioscience) with modifications to a previously described protocol (55,59). Filters were coated with either 12 µL of ice-cold basement membrane extract (4% or 20%, basement membrane invasion assay; Matrigel, BD Bioscience) or 25 µL of ice-cold collagen I (0.28 ng/µL, interstitial invasion assay; BD Bioscience). Epithelial cells were added to the upper chamber in 300 µL of serum-free medium. DOK or HSC-3 cells were seeded on 20% Matrigel-coated filters at 10^5 cells per well, whereas 4×10^5 HaCAT cells were seeded on 4% Matrigel-coated filters. For migration assays, DOK (4×10^4) or HaCAT (4×10^5) cells were seeded onto collagen I–coated filters. The lower chamber was filled with 300 µL of conditioned medium collected from tobacco-exposed or control fibroblasts and normalized to fibroblast number. After incubation for 16 or 24 h, cells were fixed with 2.5% glutaraldehyde in PBS and stained with 0.5% toluidine blue in 2% Na_2CO_3. Cells that remained in the gel were removed with cotton tips. Cells on the underside of the filter were counted using light microscopy.

Skin Rafts

To prepare artificial skin constructs (RAFT), 1×10^6 human dermal fibroblasts (Cambrex) in 0.5 mL of DMEM were mixed with 6.5 mL of ice-cold neutralized (pH 7) rat tail collagen (4.07 mg/mL), 2 mL of 5× high glucose DMEM and 1 mL of 10× reconstitution buffer (260 mmol/L sodium carbonate, 200 mmol/L HEPES, 0.05 N sodium hydroxide). Nine hundred microliters of this mixture was transferred to 12-well plates. Two hours later, 2×10^5 keratinocytes (NHEK, Cambrex) in 1 mL of keratinocyte growth medium-2 were added to the surface of the fibroblast mixture. RAFTs were cultured for 5 days with medium changes every 2 to 3 days using RAFT maintenance medium (1:1 mixture of fibroblast growth medium and keratinocyte growth medium-2). After 5 days, when the keratinocytes had reached confluence, the RAFTs were transferred to Petri dishes containing an elevated sterile stainless steel mesh to expose the keratinocytes to an air-water interface. The dishes were filled with RAFT maintenance medium to the level of the steel mesh. After 10 days, RAFTs were divided into three groups: 0%, 2%, and 4% Tob. The 0% group ($n = 4$) continued to receive the RAFT maintenance medium. The 2% group ($n = 3$) received RAFT maintenance medium + 2% Tob, and the 4% group ($n = 3$) received RAFT maintenance medium + 4% Tob. The medium was changed every 3 to 5 days. After 30 days, RAFTs were fixed in 4% buffered paraformaldehyde

overnight and immersed in sucrose prior to freezing in embedding solution (OCT, Sakura) and sectioning. Immunostaining was done as previously described above.

Statistical Analysis

Unless otherwise indicated, the experiments were done at least twice or thrice, and the values represent the mean of three to five samples and SD around the mean. Significant differences were also determined using the unpaired Student's *t* test, where suitable. *P* < 0.05 defined statistical significance.

Acknowledgments

References

1. NIH-NCI cancer rates and risks. Vol. 4th ed.. 1996. p. 67-72.

2. Hunter KD, Parkinson EK, Harrison PR. Profiling early head and neck cancer. Nat Rev Cancer 2005;5:127–135. [PubMed: 15685196]

3. Bagchi M, Balmoori J, Bagchi D, Stohs SJ, Chakrabarti J, Das DK. Role of reactive oxygen species in the development of cytotoxicity with various forms of chewing tobacco and pan masala. Toxicology 2002;179:247–255. [PubMed: 12270596]

4. Hecht SS. Tobacco carcinogens, their biomarkers and tobacco-induced cancer. Nat Rev Cancer 2003;3:733–744. [PubMed: 14570033]

5. De Flora S, D'Agostini F, Balansky R, et al. Modulation of cigarette smoke-related end-points in mutagenesis and carcinogenesis. Mutat Res 2003;523–4:237–252.

6. Maciag A, Bialkowska A, Espiritu I, et al. Gestation stage-specific oxidative deoxyribonucleic acid damage from sidestream smoke in pregnant rats and their fetuses. Arch Environ Health 2003;58:238–244. [PubMed: 14655905]

7. Bagchi M, Balmoori J, Bagchi D, Ray SD, Kuszynski C, Stohs SJ. Smokeless tobacco, oxidative stress, apoptosis, and antioxidants in human oral keratinocytes. Free Radic Biol Med 1999;26:992–1000. [PubMed: 10232844]

8. Yildiz D, Liu YS, Ercal N, Armstrong DW. Comparison of pure nicotine- and smokeless tobacco extract-induced toxicities and oxidative stress. Arch Environ Contam Toxicol 1999;37:434–439. [PubMed: 10508890]

9. Hoffmann D, Adams JD. Carcinogenic tobacco-specific N-nitrosamines in snuff and in the saliva of snuff dippers. Cancer Res 1981;41:4305–4308. [PubMed: 7198005]

10. Hecht SS. Biochemistry, biology, and carcinogenicity of tobacco-specific N-nitrosamines. Chem Res Toxicol 1998;11:559–603. [PubMed: 9625726]

11. Yin L, Morita A, Tsuji T. Alterations of extracellular matrix induced by tobacco smoke extract. Arch Dermatol Res 2000;292:188–194. [PubMed: 10836612]

12. Kim HJ, Liu X, Wang H, et al. Glutathione prevents inhibition of fibroblast-mediated collagen gel contraction by cigarette smoke. Am J Physiol Lung Cell Mol Physiol 2002;283:L409–L417. [PubMed: 12114203]

13. Van Schooten FJ, Nia AB, De Flora S, et al. Effects of oral administration of N-acetyl-L-cysteine: a multi-biomarker study in smokers. Cancer Epidemiol Biomarkers Prev 2002;11:167–175. [PubMed: 11867504]

14. DePinho RA. The age of cancer. Nature 2000;408:248–254. [PubMed: 11089982]

15. Tlsty TD. Stromal cells can contribute oncogenic signals. Semin Cancer Biol 2001;11:97–104. [PubMed: 11322829]

16. Wilson SE, Netto M, Ambrosio R Jr. Corneal cells: chatty in development, homeostasis, wound healing, and disease. Am J Ophthalmol 2003;136:530–536. [PubMed: 12967809]

17. Olumi AF, Grossfeld GD, Hayward SW, Carroll PR, Tlsty TD, Cunha GR. Carcinoma-associated fibroblasts direct tumor progression of initiated human prostatic epithelium. Cancer Res 1999;59:5002–5011. [PubMed: 10519415]

18. Kuperwasser C, Chavarria T, Wu M, et al. Reconstruction of functionally normal and malignant human breast tissues in mice. Proc Natl Acad Sci U S A 2004;101:4966–4971. [PubMed: 15051869]

19. Barcellos-Hoff MH, Ravani SA. Irradiated mammary gland stroma promotes the expression of tumorigenic potential by unirradiated epithelial cells. Cancer Res 2000;60:1254–1260. [PubMed: 10728684]

20. Tipton DA, Dabbous MK. Effects of nicotine on proliferation and extracellular matrix production of human gingival fibroblasts *in vitro*. J Periodontol 1995;66:1056–1064. [PubMed: 8683418]

21. Wang Y, Rotem E, Andriani F, Garlick JA. Smokeless tobacco extracts modulate keratinocyte and fibroblast growth in organotypic culture. J Dent Res 2001;80:1862–1866. [PubMed: 11926249]

22. Giannopoulou C, Roehrich N, Mombelli A. Effect of nicotine-treated epithelial cells on the proliferation and collagen production of gingival fibroblasts. J Clin Periodontol 2001;28:769–775. [PubMed: 11442737]

23. Dimri GP, Lee X, Basile G, et al. A biomarker that identifies senescent human cells in culture and in aging skin *in vivo*. Proc Natl Acad Sci U S A 1995;92:9363–9367. [PubMed: 7568133]

24. Nair J, Ohshima H, Nair UJ, Bartsch H. Endogenous formation of nitrosamines and oxidative DNA-damaging agents in tobacco users. Crit Rev Toxicol 1996;26:149–161. [PubMed: 8688158]

25. Davies KJ. The broad spectrum of responses to oxidants in proliferating cells: a new paradigm for oxidative stress. IUBMB Life 1999;48:41–47. [PubMed: 10791914]

26. Chen QM, Bartholomew JC, Campisi J, Acosta M, Reagan JD, Ames BN. Molecular analysis of H2O2-induced senescent-like growth arrest in normal human fibroblasts: p53 and Rb control G1 arrest but not cell replication. Biochem J 1998;332:43–50. [PubMed: 9576849]

27. Di Leonardo A, Linke SP, Clarkin K, Wahl GM. DNA damage triggers a prolonged p53-dependent G1 arrest and long-term induction of Cip1 in normal human fibroblasts. Genes Dev 1994;8:2540–2551. [PubMed: 7958916]

28. Bassing CH, Alt FW. H2AX may function as an anchor to hold broken chromosomal DNA ends in close proximity. Cell Cycle 2004;3:149–153. [PubMed: 14712078]

29. Takai H, Smogorzewska A, de Lange T. DNA damage foci at dysfunctional telomeres. Curr Biol 2003;13:1549–1556. [PubMed: 12956959]

30. d'Adda di Fagagna F, Reaper PM, Clay-Farrace L, et al. A DNA damage checkpoint response in telomere-initiated senescence. Nature 2003;426:194–198. [PubMed: 14608368]

31. Brugarolas J, Moberg K, Boyd SD, Taya Y, Jacks T, Lees JA. Inhibition of cyclin-dependent kinase 2 by p21 is necessary for retinoblastoma protein-mediated G1 arrest after γ-irradiation. Proc Natl Acad Sci U S A 1999;96:1002–1007. [PubMed: 9927683]

32. Wolf FI, Torsello A, Covacci V, et al. Oxidative DNA damage as a marker of aging in WI-38 human fibroblasts. Exp Gerontol 2002;37:647–656. [PubMed: 11909682]

33. Vile GF. Active oxygen species mediate the solar ultraviolet radiation-dependent increase in the tumour suppressor protein p53 in human skin fibroblasts. FEBS Lett 1997;412:70–74. [PubMed: 9257692]

34. Campisi J. Senescent cells, tumor suppression, and organismal aging: good citizens, bad neighbors. Cell 2005;120:513–522. [PubMed: 15734683]

35. Ishii T, Matsuse T, Igarashi H, Masuda M, Teramoto S, Ouchi Y. Tobacco smoke reduces viability in human lung fibroblasts: protective effect of glutathione S-transferase P1. Am J Physiol Lung Cell Mol Physiol 2001;280:L1189–L1195. [PubMed: 11350797]

36. Dilley TK, Bowden GT, Chen QM. Novel mechanisms of sublethal oxidant toxicity: induction of premature senescence in human fibroblasts confers tumor promoter activity. Exp Cell Res 2003;290:38–48. [PubMed: 14516786]

37. West MD, Pereira-Smith OM, Smith JR. Replicative senescence of human skin fibroblasts correlates with a loss of regulation and overexpression of collagenase activity. Exp Cell Res 1989;184:138–147. [PubMed: 2551704]

38. Campisi J, d'Adda di Fagagna F. Cellular senescence: when bad things happen to good cells. Nat Rev Mol Cell Biol 2007;8:729–740. [PubMed: 17667954]

39. Zeng G, Millis AJ. Differential regulation of collagenase and stromelysin mRNA in late passage cultures of human fibroblasts. Exp Cell Res 1996;222:150–156. [PubMed: 8549657]

40. Millis AJ, Hoyle M, McCue HM, Martini H. Differential expression of metalloproteinase and tissue inhibitor of metalloproteinase genes in aged human fibroblasts. Exp Cell Res 1992;201:373–379. [PubMed: 1322316]

41. Krtolica A, Parrinello S, Lockett S, Desprez PY, Campisi J. Senescent fibroblasts promote epithelial cell growth and tumorigenesis: a link between cancer and aging. Proc Natl Acad Sci U S A 2001;98:12072–12077. [PubMed: 11593017]

42. Parrinello S, Coppe J-P, Krtolica A, Campisi J. Stromal-epithelial interactions in aging and cancer: senescent fibroblasts alter epithelial cell differentiation. J Cell Sci 2005;118:485–496. [PubMed: 15657080]

43. Wang X, Hao T, Wu R. Effect of cigarette smoke extract on E-cadherin expression of airway epithelial cells. Zhonghua Jie He He Hu Xi Za Zhi 1999;22:414–416. [PubMed: 11775814]

44. Boucher RC, Johnson q, Inoue S, Hulbert W, Hogg JC. The effect of cigarette smoke on the permeability of guinea pig airways. Lab Invest 1980;43:94–100. [PubMed: 7392577]

45. Hasegawa M, Nelson HH, Peters E, Ringstrom E, Posner M, Kelsey KT. Patterns of gene promoter methylation in squamous cell cancer of the head and neck. Oncogene 2002;21:4231–4236. [PubMed: 12082610]

46. Wood B, Leong A. The biology and diagnostic applications of cadherins in neoplasia: a review. Pathology 2003;35:101–105. [PubMed: 12745455]

47. Hirohashi S, Kanai Y. Cell adhesion system and human cancer morphogenesis. Cancer Sci 2003;94:575–581. [PubMed: 12841864]

48. Thomas GJ, Speight PM. Cell adhesion molecules and oral cancer. Crit Rev Oral Biol Med 2001;12:479–498. [PubMed: 11806518]

49. Nobukuni S, Watanabe K, Inoue J, Wen FQ, Tamaru N, Yoshida M. Cigarette smoke inhibits the growth of lung fibroblasts from patients with pulmonary emphysema. Respirology 2002;7:217–223. [PubMed: 12153687]

50. Nyunoya T, Monick MM, Klingelhutz A, Yarovinsky TO, Cagley JR, Hunninghake GW. Cigarette smoke induces cellular senescence. Am J Respir Cell Mol Biol 2006;35:681–688. [PubMed: 16840774]

51. Hecht SS. DNA adduct formation from tobacco-specific N-nitrosamines. Mutat Res 1999;424:127–142. [PubMed: 10064856]

52. DeMarini DM. Genotoxicity of tobacco smoke and tobacco smoke condensate: a review. Mutat Res 2004;567:447–474. [PubMed: 15572290]

53. Chang SE, Foster S, Betts D, Marnock WE. DOK, a cell line established from human dysplastic oral mucosa, shows a partially transformed non-malignant. Int J Cancer 1992;52:896–902. [PubMed: 1459732]

54. Skobe M, Fusenig NE. Tumorigenic conversion of immortal human keratinocytes through stromal cell activation. Proc Natl Acad Sci U S A 1998;95:1050–1055. [PubMed: 9448283]

55. Matsumoto K, Horikoshi M, Rikimaru K, Enomoto S. A study of an *in vitro* model for invasion of oral squamous cell carcinoma. J Oral Pathol Med 1989;18:498–501. [PubMed: 2607470]

56. Park NH, Akoto-Amanfu E, Paik DI. Smokeless tobacco carcinogenesis: the role of viral and other factors. CA Cancer J Clin 1988;38:248–256. [PubMed: 2840179]

57. Parrinello S, Samper E, Krtolica A, Goldstein J, Melov S, Campisi J. Oxygen sensitivity severely limits the replicative lifespan of murine fibroblasts. Nat Cell Biol 2003;5:741–747. [PubMed: 12855956]

58. Helma C, Uhl M. A public domain image-analysis program for the single-cell gel-electrophoresis (comet) assay. Mutat Res 2000;466:9–15. [PubMed: 10751720]

59. Krtolica A, Ludlow JW. Hypoxia arrests ovarian carcinoma cell cycle progression, but invasion is unaffected. Cancer Res 1996;56:1168–1173. [PubMed: 8640779]

60. Krtolica A, Ortiz de Solorzano C, Lockett S, Campisi J. Quantification of epithelial cells in coculture with fibroblasts by fluorescence image analysis. Cytometry 2002;49:73–82. [PubMed: 12357463]
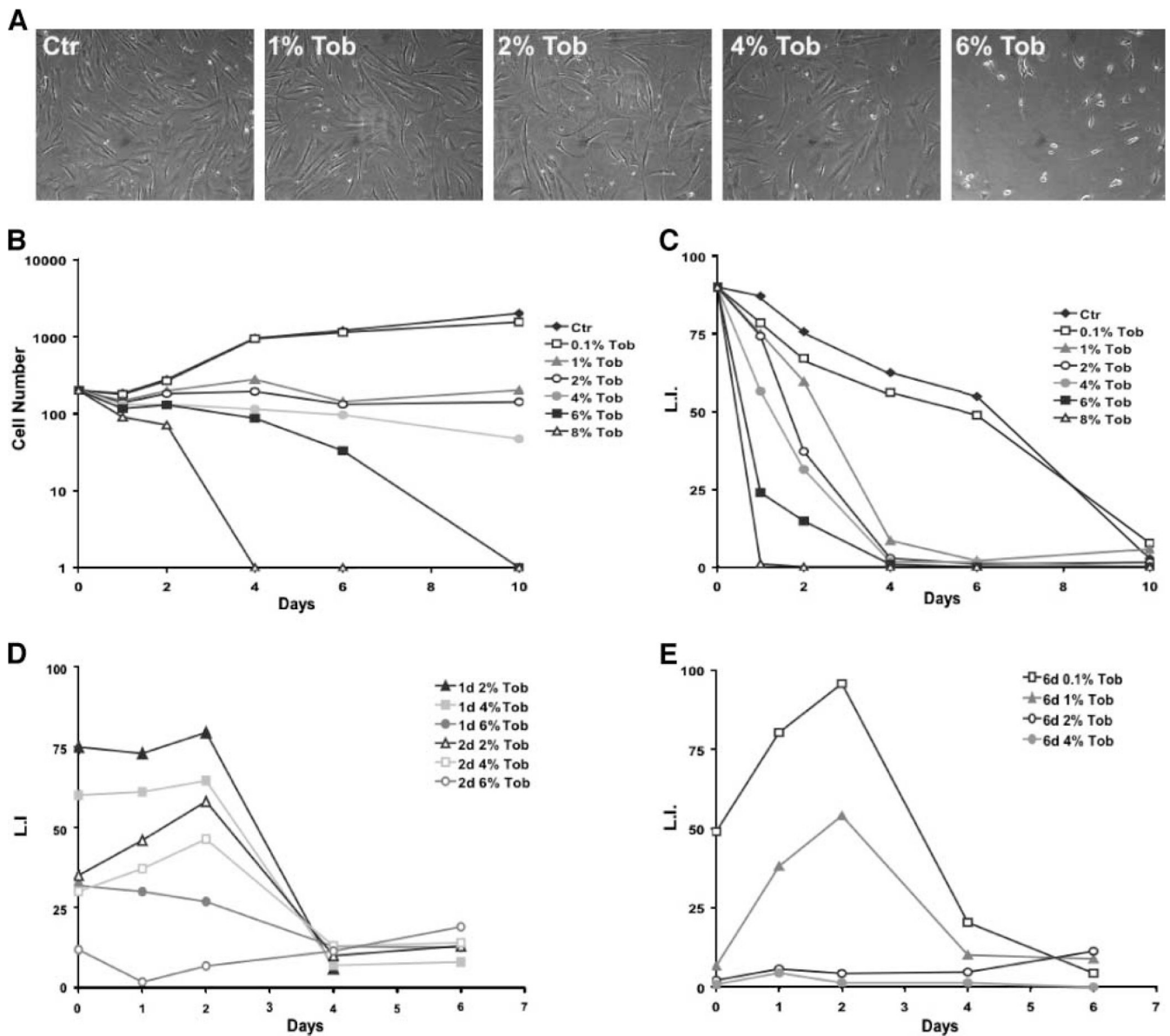
FIGURE 1.
Effects of smokeless tobacco extracts on the growth of human fibroblasts. Fibroblasts were exposed to 0 (control, *Ctr*), 1%, 2%, 4%, or 6% tobacco extract (*Tob*) and photographed 4 d later by phase contrast microscopy (**A**). Cell proliferation was followed by measuring total cell number (**B**) and [^{3}H]thymidine incorporation (**C–E**) after tobacco exposure (**B** and **C**) or after tobacco exposure followed by replacement with control medium (2-d exposure, **D**; and 6-d exposure, **E**). At least 400 cells from randomly chosen fields were quantified for each data point.
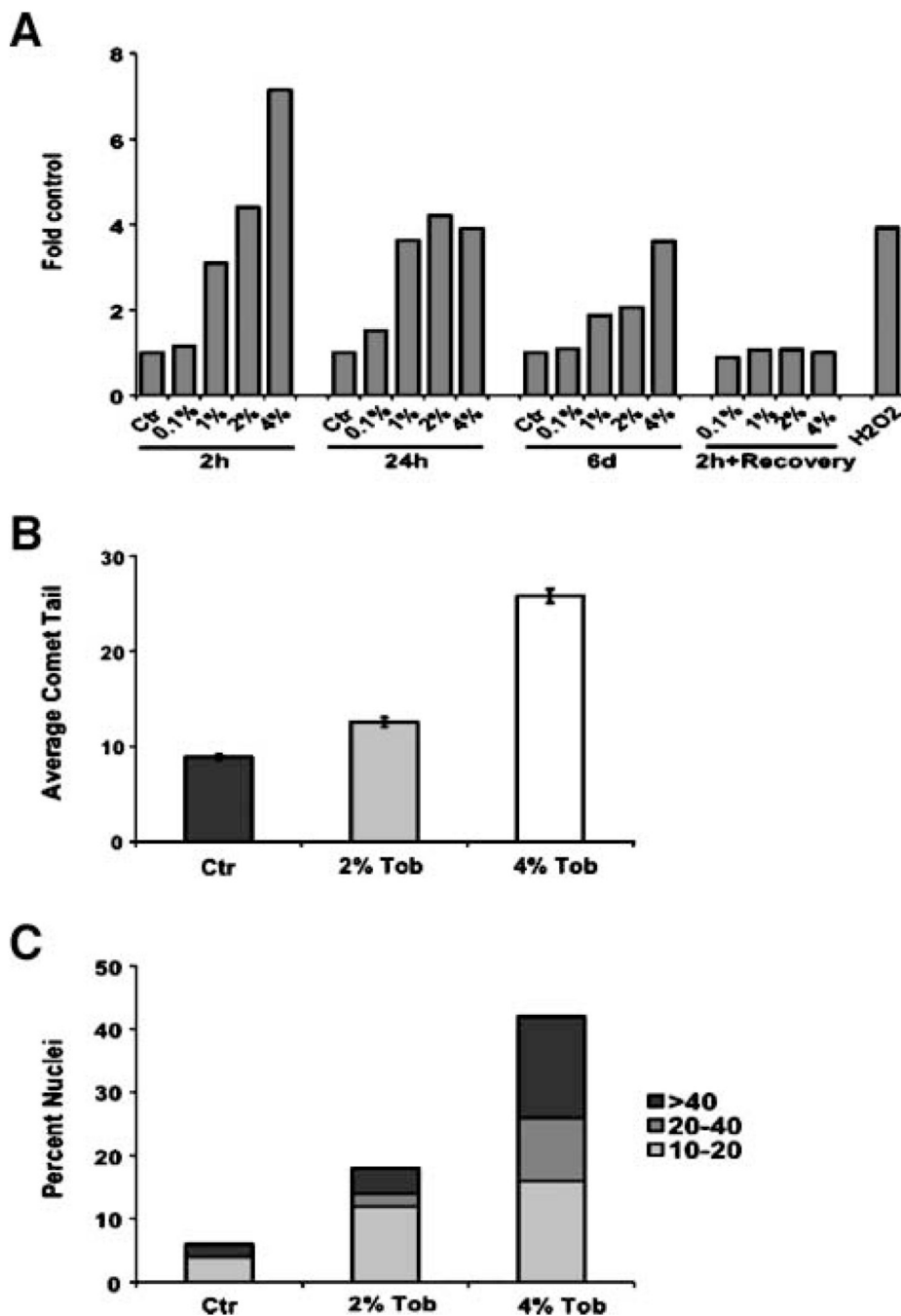
FIGURE 2.
ROS production and oxidative DNA damage in smokeless tobacco extracts – exposed fibroblasts. Intracellular ROS levels were measured by carboxy-H2DCFDA fluorescence and flow cytometry after exposure to 0 (*Ctr*), 0.1%, 1%, 2%, or 4% of Tob for 2 h, 24 h, or 6 d, or 2 h followed by 24 h recovery in Tob-free medium (**A**). Oxidative DNA damage was measured using the Fpg-FLARE comet assay and depicted as the average comet tail (**B**) and the distribution of normalized mean tail lengths (**C**). Tail lengths were normalized by subtracting the mean tail length of the untreated sample from that of the Fpg-treated sample. At least 50 randomly chosen comet tails were analyzed per duplicate sample.
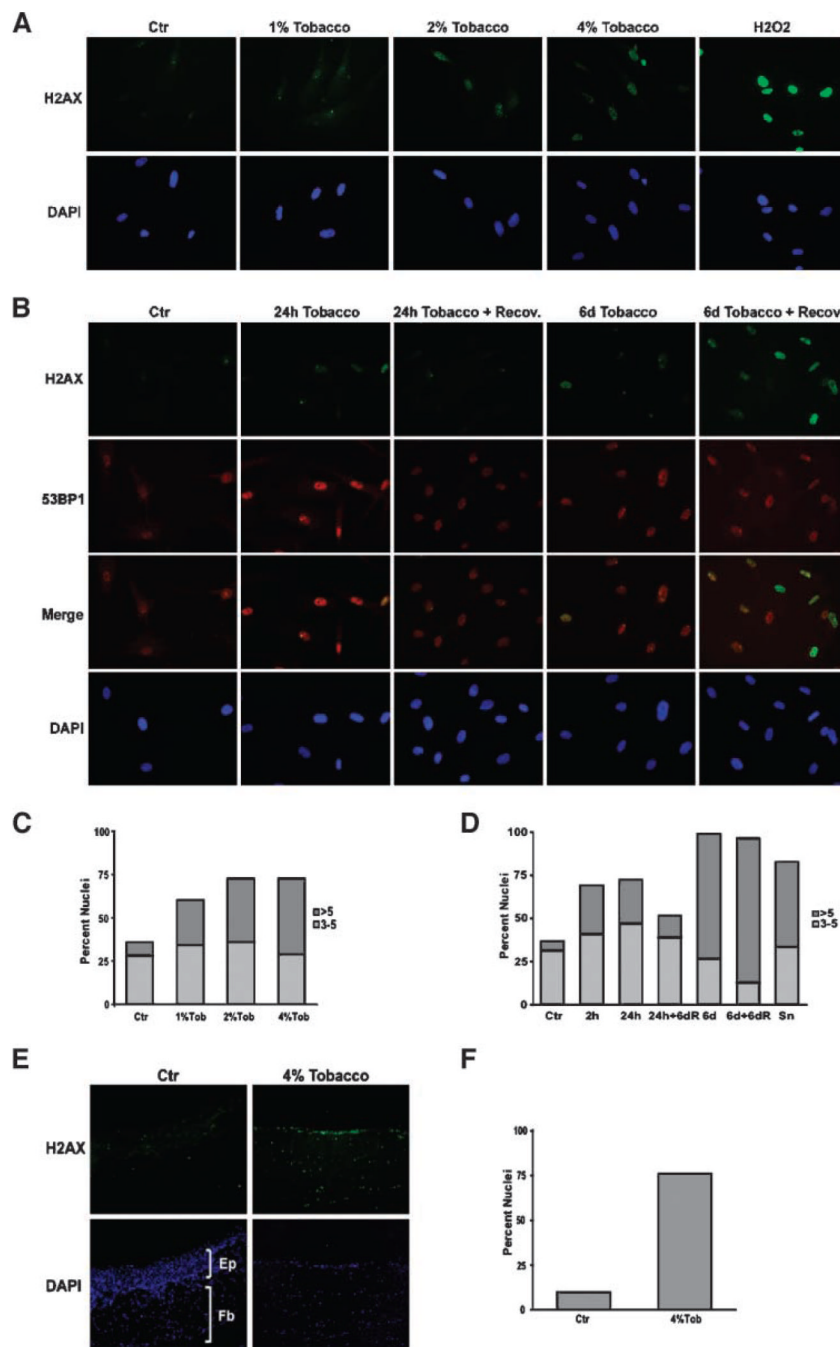
FIGURE 3.
Presence of H2AX foci in fibroblasts and skin rafts during smokeless tobacco extracts –
exposure and recovery. Fibroblasts were exposed to 0%, 1%, 2%, or 4% of Tob for 6 d (**A** and
C), or 4% tobacco extracts for 2 h, 24 h, or 6 d with or without a 6-d recovery (**B** and **D**), and
immunostained for γH2AX foci. Hydrogen peroxide – treated fibroblasts were used as a
positive control (H$_2$O$_2$). Immunostaining was done as described in Materials and Methods
(**A**, **B**, and **E**). Quantification was done manually under the epifluorescent microscope (**C**, **D**,
and **F**). At least 200 cells from randomly chosen fields were quantified for each data point.
Differentiated skin rafts were exposed to 0% or 4% of Tob for 30 d and then subjected to

γH2AX immunostaining(**E** and **F**). Representative sections for control (*Ctr*) and 4% Tob-treated samples were quantified (**F**).
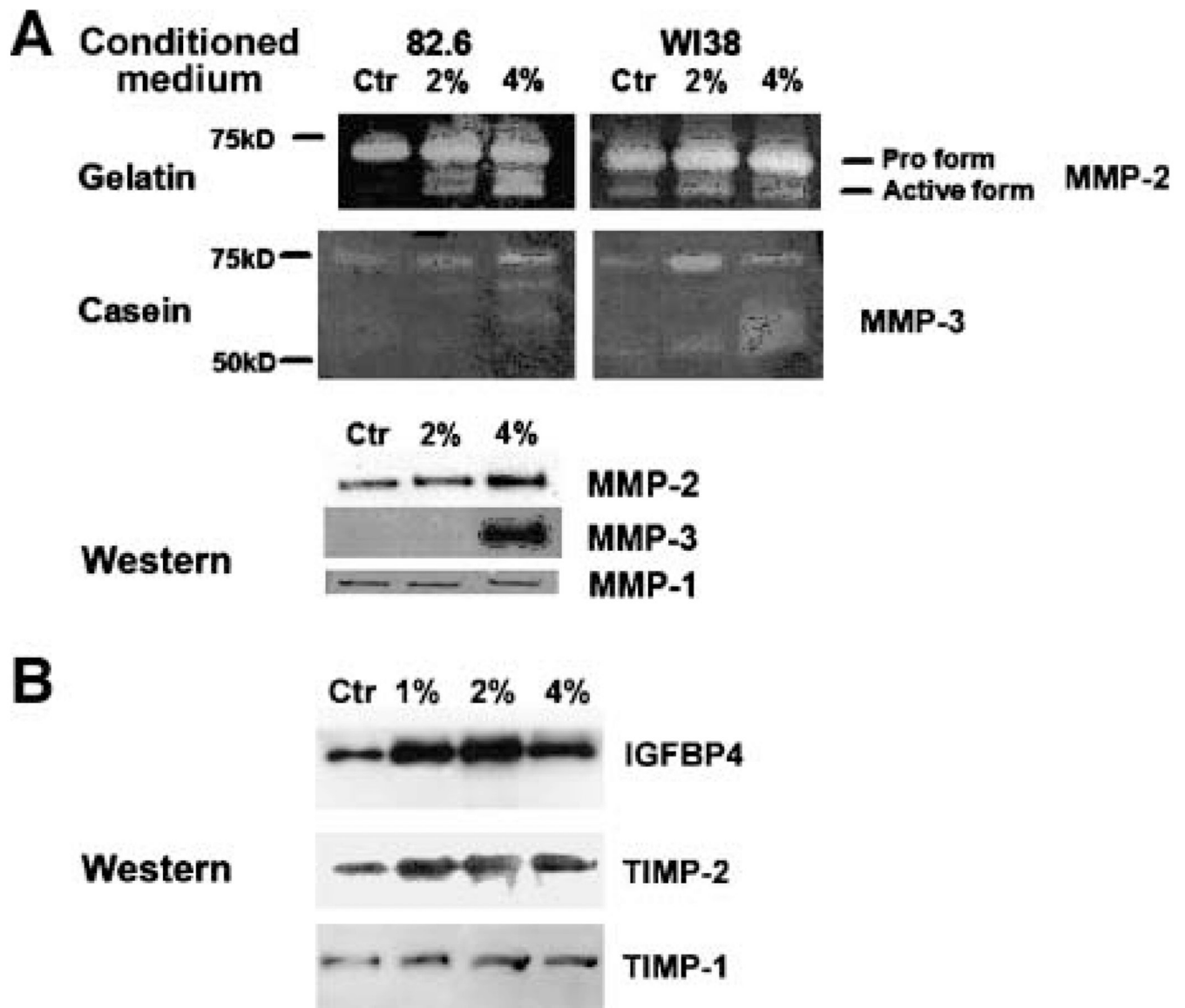
FIGURE 4.
Analysis of the smokeless tobacco extracts – induced secretory phenotype. Concentrated conditioned medium from control (*Ctr*) or tobacco-treated 82.6 and WI-38 fibroblasts were normalized to the cell number and used for gelatin and casein substrate zymography for detection of MMP-2 and MMP-3 activity, respectively, and Western blottingfor MMP-1, MMP-2, and MMP-3 (**A**). Conditioned medium was also analyzed for IGFBP4, TIMP-2, and TIMP-1 by Western blotting(**B**).
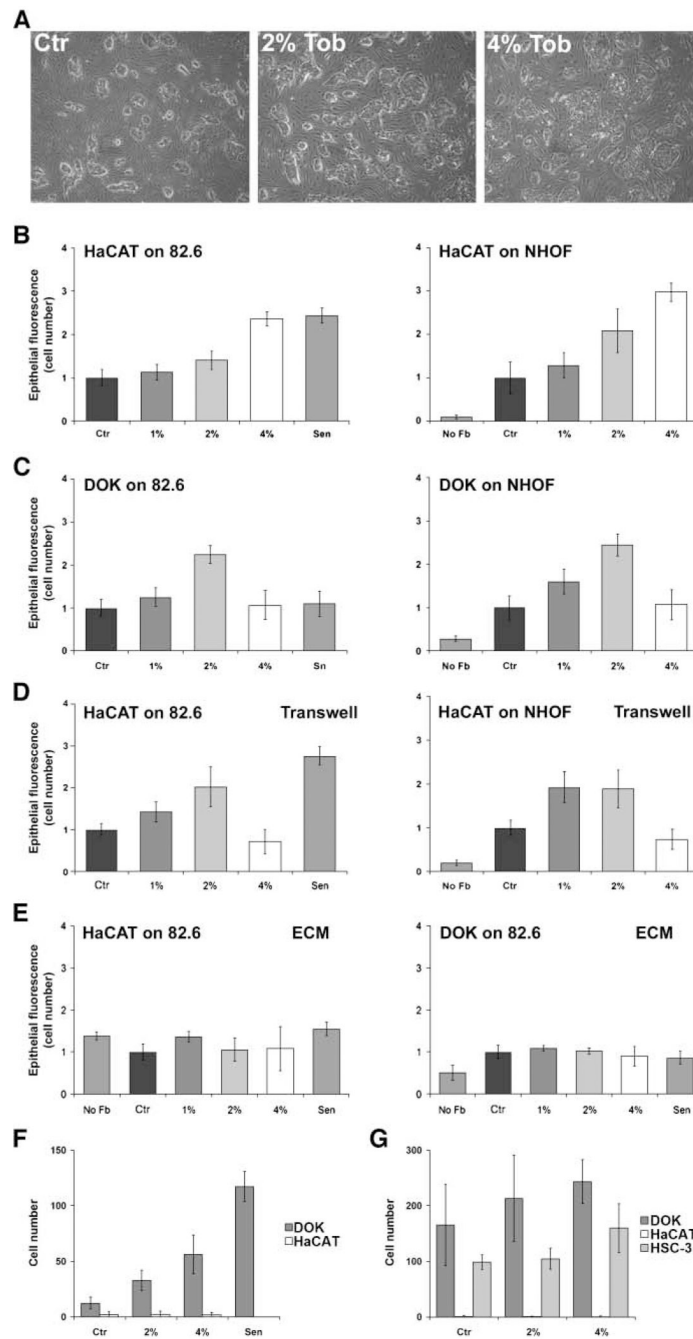
FIGURE 5.
Effect of smokeless tobacco extracts – exposed fibroblasts on keratinocyte proliferation and interstitial and basement membrane invasion. **A**. Representative fields of HaCAT cells grown in coculture with control, 2%, or 4% Tob-exposed oral fibroblasts. **B**. HaCAT keratinocytes were seeded onto 82.6 (*left*) or NHOF (*right*) fibroblasts treated with indicated concentration of Tob. Keratinocyte proliferation (epithelial fluorescence/cell number) was quantified as described in Materials and Methods after 8 d and expressed as the fold increase over control fibroblasts (*Ctr*), which received no Tob. Keratinocyte proliferation on replicatively senescent 82.6 fibroblasts (*Sen*) is shown for comparison. **C**. DOK keratinocytes were seeded onto 82.6 (*left*) or NHOF (*right*) fibroblasts and monitored for proliferation as described for **B**. **D**. HaCAT

cells were plated in the upper chamber of transwells, with 82.6 (*left*) or NHOF (*right*), treated as indicated, in the lower chambers. Keratinocytes were monitored for proliferation, as described for **B**. **E**. HaCAT (*left*) and DOK (*right*) were seeded on extracellular matrix prepared from 82.6 fibroblasts, treated as indicated, and monitored for proliferation as described in **B**. **F**. DOK (*dark gray columns*) and HaCAT (*white columns*) keratinocytes were seeded onto collagen-coated filters above wells containing conditioned medium from 82.6 dermal fibroblasts treated with 0% (*Ctr*) to 4% Tob or replicatively senescent (*Sen*). After 16 h, the number of keratinocytes that invaded through the collagen gel to the other side of the membrane was quantified. **G**. DOK, HaCAT, and HCS-3 (*light gray columns*; invasive positive control) keratinocytes were seeded onto Matrigel-coated filters above wells containing conditioned medium from 82.6 dermal fibroblasts treated with 0% (*Ctr*) to 4% Tob. The number of keratinocytes that invaded through the Matrigel to the other side of the membrane was quantified. Columns, mean of three to five samples from independently confirmed representative experiments; bars, SD.
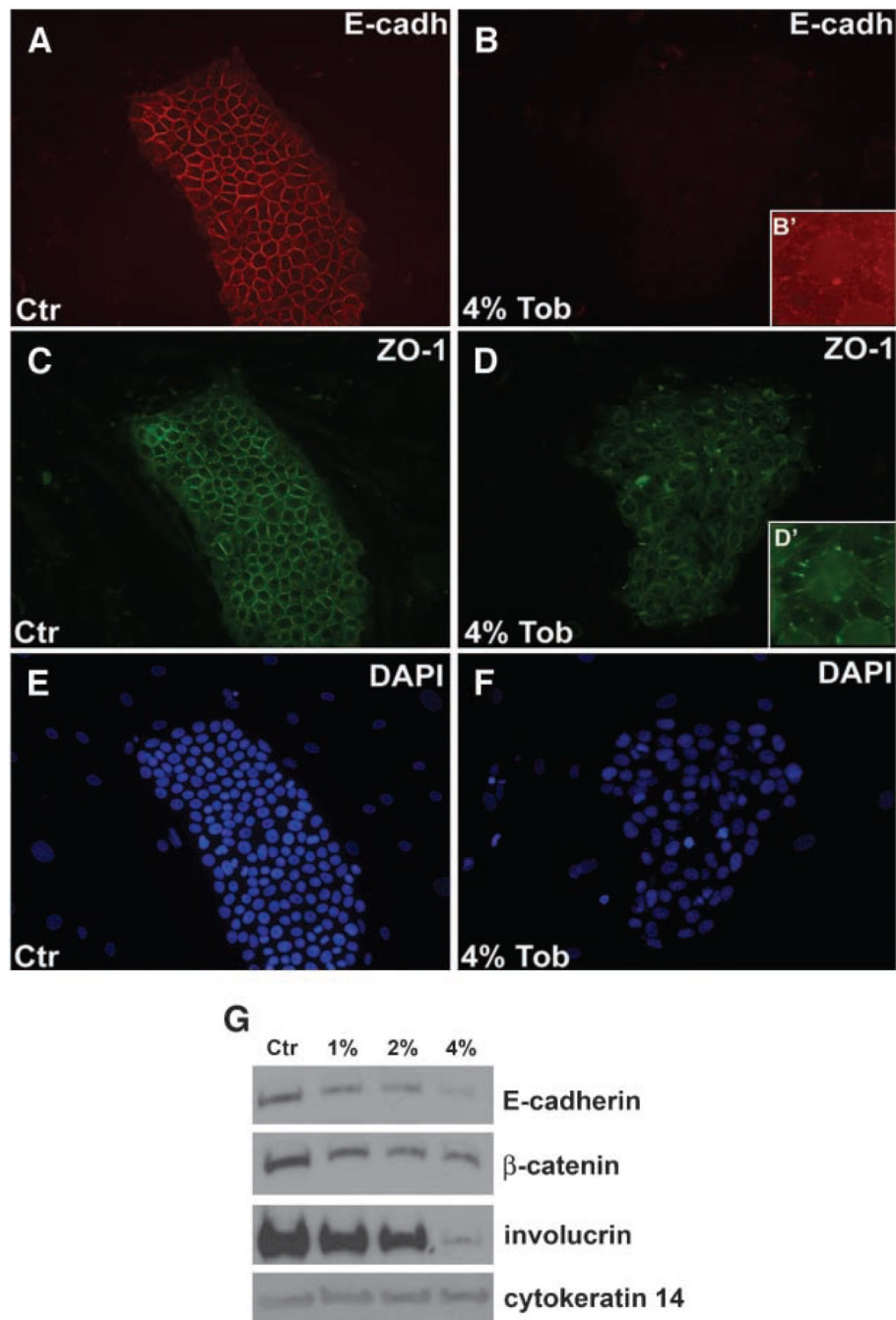
FIGURE 6.
Changes in epithelial cell-cell interactions in cocultures with smokeless tobacco extracts –
exposed fibroblasts. HaCAT colonies on control (**A**, **C**, and **E**) or 4% Tob-exposed (**B**, **D**, and
F) 82.6 dermal fibroblasts were immunostained for E-cadherin (**A** and **B**), ZO-1 (**C** and **D**),
and nuclei (DAPI; **E** and **F**). Cocultures of HaCAT and 1%, 2%, or 4% Tob-exposed fibroblasts
were also harvested for Western blotting(**G**).

Table 1

Conditioned Medium were Analyzed Using Anti-body Arrays

	Control	1% Tob	2% Tob	4% Tob
sTNF RII	++	+	+/−	+/−
IGFBP3	−	−	−	+
uPAR	−	−	−	+
Angiogenin	−	−	−	−
GCSF	−	−	−	−
RANTES	+/−	+/−	+/−	+/−
GRO	−	−	+/−	+
IL-1ra	+	+	++	++
bFGF	−	−	+	+
MIP-1a	+	+	+	+
ICAM-1	−	−	−	+
Osteoprotegerin	−	+	+	+
IGFBP4	+	++	+++	++
IL-6	+	+	+	+++
MCP-1	+/−	+	++	++
TIMP-1	+	++	++	++
IL-8	+/−	++	++	++
TIMP-2	+	+++	+++	+++

NOTE: Secreted proteins significantly up-regulated by Tob are designated +, ++, or +++ (also indicated by progressively darker shading), whereas proteins showing little or no change are designated +/− or −.

Table 2

Quantification of E-Cadherin, β-Catenin,and Involucrin Expression in Epithelial Cells Was Achieved by Normalizing to the Epithelial-Specific Cytoskeleton Protein Cytokeratin-14

	Control	1% Tob	2% Tob	4% Tob
E-Cadherin	100	42	32	5
β-Catenin	100	49	36	31
Involucrin	100	70	58	8